Smart Structures and Systems, *Vol. 27, No. 2 (2021) 157-172*
DOI: https://doi.org/10.12989/sss.2021.27.2.157

Amplitude-dependent model updating of masonry buildings undergoing demolition

Panagiotis Martakis*, Yves Reuland [a] and Eleni Chatzi [b]

ETH Zurich (Department of Civil, Environmental and Geomatic Engineering, Chair of Structural Mechanics and Monitoring, Zurich, Switzerland)

(*Received July 21, 2020, Revised September 7, 2020, Accepted September 16, 2020*)

Abstract. Precise knowledge of dynamic characteristics and data-driven inference of material properties of existing buildings are key for assessing their seismic capacity. While dynamic measurements on existing buildings are typically extracted under ambient conditions, masonry, in particular, exhibits nonlinear behavior at already very low shaking amplitudes. This implies that material properties, inferred via data-driven model updating under ambient conditions, may be inappropriate for predicting behavior under seismic actions. In addition, the relative amount of nonlinearity arising from structural behavior and soil-structure interaction are often unknown. In this work, Bayesian model updating is carried out on field measurements that are representative of increasing levels of shaking, as induced during demolition, on a pre-code masonry building. The results demonstrate that masonry buildings exhibit nonlinear behavior as the elastic modulus drops by up to 18% in the so-called equivalent elastic range, in which the observed frequency drop is reversible, prior to any visible sign of damage. The impact of this effect on the seismic assessment of existing structures is investigated via a nonlinear seismic analysis of the examined case study, calibrated under dynamic recordings of varying response amplitude. While limited to a single building, such changes in the inferred material properties results in a significant reduction of the safety factor, in this case by 14%.

Keywords: structural health monitoring; forced testing under demolition; output-only modal identification; amplitude-dependent stiffness; existing masonry buildingsl non-linear behavior

1. Introduction

Earthquakes continue to comprise one of the deadliest natural hazards, with the majority of the casualties caused by collapsing buildings (Kenny 2009). While much effort has been made to improve building codes and new structures can arguably be considered earthquake-safe, existing buildings often fail to comply with modern seismic code prescriptions. Among building typologies, masonry buildings stand out as the most vulnerable (Lourenço and Roque 2006, Lam *et al*. 2019). Repairing or even replacing all existing buildings that have been built prior to current design codes is economically impossible and environmentally unsustainable, given that the construction industry is already the largest producer of solid waste (World Economic Forum 2016). Better knowledge of the behavior of existing structures may justify the extension of their lifespan without compromising the resilience of communities with respect to natural disasters.

Structural health monitoring (SHM), which relies on utilization of sensor data from operating structures, has the potential to expand our knowledge concerning performance of existing buildings, as a supplement to laboratory-based experimentation (Spencer *et al*. 2004a, Ma and Li 2015, Chatzis *et al*. 2015 and Stavridis *et al*. 2011), and possibly alleviating destructive testing and supporting lifetime safe exploitation of novel structural solutions (Bedon 2019). Rapid developments in sensor technology and the broad establishment of the Internet-of-Things (IoT) enriched the arsenals of structural sensing tools for structures under seismic risk, overcoming most of the main challenges that prohibited the broad application of smart sensor networks for SHM applications in the past 20 years (Spencer *et al*. 2004b).

Works related to the use of SHM, for dynamic characterization and monitoring of buildings, typically exploit vibration measurements to infer the modal characteristics of the examined system, either as a proxy of structural health (Gattulli *et al*. 2013, Vidal *et al*. 2014, Cheng *et al*. 2015) or for further exploitation in inverse parameter updating of computational models (Atamturktur and Laman 2012, Lam *et al*. 2019, Lombaert *et al*. 2009, Reuland *et al*. 2019a). Other applications of vibration monitoring relate to slender structures, where the serviceability requirements are more restrictive than safety limits. In such cases, vibrational monitoring supports the validation of modeling assumptions and the evaluation of compliance to code prescriptions (Martakis *et al*. 2019). Finally, problems related to oscillating machinery and its effect on the foundation impedance, form another field of extensive academic research, which could profit from better

*Corresponding author, Ph.D. Student,
E-mail: martakis@ibk.baug.ethz.ch
[a] Ph.D., E-mail: reuland@ibk.baug.ethz.ch
[b] Professor, E-mail: chatzi@ibk.baug.ethz.ch

ISSN: 1738-1584 (Print), 1738-1991 (Online)

knowledge of vibration responses (Gazetas 1992).

Ideally, building dynamics are measured under actual seismic events (Ulusoy *et al*. 2010), or under forced excitation (Yu *et al*. 2006, Steiger *et al*. 2015). Soyoz *et al*. (2013) employed an eccentric mass shaker to mobilize a reinforced concrete building prior to and after retrofitting, with the aim of assessing the efficacy of the retrofitting solution. However, various technical and administrative complications undermine such controlled shaking experiments for testing of real structures, with perhaps a primary obstacle lying in the need to suspend the function of the tested infrastructure, or building. As a result, output-only modal identification algorithms (Brincker *et al*. 2001, Van Overschee and De Moor 1996) for structures that are subjected to ambient excitation present a more attractive, if not the only, alternative for dynamic measurements. However, methodologies that involve ambient vibrations are inevitably limited to the structural response in the commonly assumed linear elastic range, which may not be representative of structural behavior under high-amplitude loads (Astorga *et al*. 2018). This limitation becomes even more prominent for masonry structures (Michel *et al*. 2011, Ceravolo *et al*. 2017) that exhibit non-linear behavior even at low excitation levels (order of magnitude lower than earthquake excitations). Furthermore, the effect of the soil-foundation-structure interaction (SFSI), which is proven to substantially affect the dynamic response of low-rise buildings (Martakis *et al*. 2017), cannot be captured by considering only ambient excitation. This paper proposes a testing and analysis framework for model updating based on dynamic measurements whose amplitude lies beyond the range of classical ambient vibrations, which typically do not exceed amplitudes of 0.1 mg. Thus, changes in modal parameters, such as frequencies, mode-shapes and equivalent viscous damping, due to changes in response amplitude are captured.

With the development and availability of structural sensing options, significant research efforts have been devoted to solve the inverse model updating problem based on measurement data (Jaishi and Ren 2005, Foti *et al*. 2014, Altunişik *et al*. 2018). To tackle uncertainties that are inherent in measurements and are further exacerbated due to the simplifications adopted in physics-based models, a model-updating framework based on Bayesian conditional probability has been proposed by Beck and Katafygiotis (1998). Although certain limitations of Bayesian model-updating schemes and the underlying uncertainty structure have been reported (Tarantola 2006, Reuland *et al*. 2017a, Pai *et al*. 2019), this approach forms a potent tool for solving the inverse updating problem (Beck and Au 2002, Vanik *et al*. 2000, Lam *et al*. 2016, Papadimitriou *et al*. 2011, Cheung and Beck 2009, Jensen *et al*. 2014, Straub and Papaioannou 2015).

Typical model-updating approaches for buildings consider fixed boundary conditions (Bakir *et al*. 2007, Behmanesh *et al*. 2017, Bartoli *et al*. 2017) and thus, ignore the SFSI effect. Updating such models, without considering the uncertainties from amplitude-dependent building behavior, may result in erroneous predictions that can lead to either unnecessary recommendation or unsafe neglecting of retrofitting. Song *et al*. (2019b) applied a hierarchical Bayesian model updating approach to a two-story concrete building, demonstrating the influence of the response amplitude onto the estimated parameters. Asgarieh *et al*. (2012) traced the frequency shifts and their influence on updated parameters of a linear finite-element model. However, only one contribution (Ceravolo *et al*. 2017) attempted a rigorous derivation of the amount of nonlinearity that can be attributed to the soil. A model-updating approach for both structure and soil, considering uncertainties, has not been accomplished. In this paper, excitations from planned demolition activities are used to estimate the influence amplitude-dependent dynamic properties of masonry buildings on updated parameters that describe the behavior of the soil and the structure. The subsequent utilization of updated model parameters bears a direct influence on both the simulated seismic behavior and the spectral demand and thus, on the predicted vulnerability of the structures (Snoj *et al*. 2013, Reuland *et al*. 2017b). Therefore, the influence of updated parameters on predicted non-linear lateral load bearing is assessed. Such information can provide guidance for practitioners seeking to reduce uncertainties in the seismic assessment of existing buildings through solution of the inverse problem of model updating.

This paper starts with a description of the studied building and the measurement system that are used, as well as the demolition process, which allowed to measure vibrations that exceed ambient levels without introducing permanent damage. In Section 3, the modal properties of the building in the healthy state are identified for both, ambient vibrations as well as higher levels of excitation. Subsequently, the parameter values of an equivalent-frame model are updated using a Bayesian approach and the influence of the variability in vibration amplitudes on the model-parameter identification and finally on the seismic performance are assessed.

2. Model updating with dynamic measurements at different amplitude levels

This section contains an overview of the proposed workflow for the inverse task of updating numerical models, based on dynamic measurements in a wide range of response amplitudes. The proposed workflow is demonstrated through its application to a real unreinforced masonry building, which has been equipped with acceleration sensors during planned demolition.

2.1 Case study and instrumentation

The studied building, erected in Zurich (Switzerland) in 1922, comprises two storeys and an attic with outer dimensions of 10.2 m in length and 8.0 m in width. An overview of the geometry is given in Fig. 1. The internal and external load-bearing shear walls consist of simple- and double-layered clay masonry respectively, while the floors are formed by timber beams, aligned parallel to the transverse direction of the building. The facades along the longitudinal direction, which is parallel to the street, contain

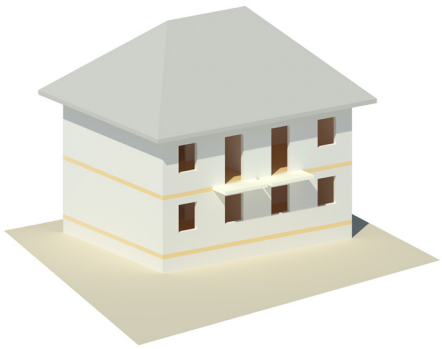

(a) Three-dimensional view. The front facade corresponds to the roadside of the building

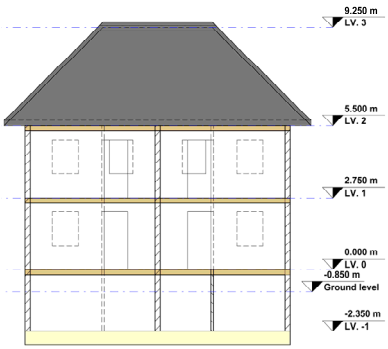

(b) Cross section. All sensor nodes were placed at the storey levels 1 and 2

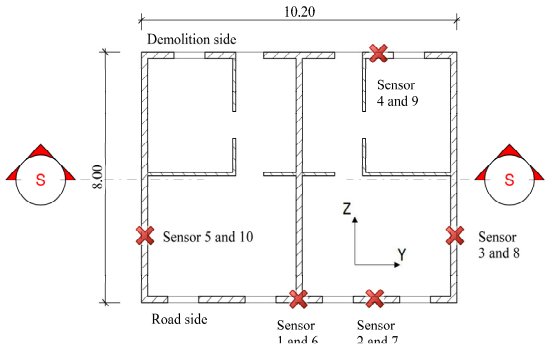

(c) Typical ground floor. The red crosses indicate the positions of the triaxial sensor nodes, at levels 1 and 2. All sensors were aligned to the main axes of the building: Y and Z

(d) Typical sensor placement

Fig. 1 Overview of the building geometry and sensor layout

openings that reduce the stiffness. The regular and symmetric geometry in plane and in elevation is common for buildings of this age, which compose today a substantial part of the residential building stock in Switzerland and central Europe in general (Crowley *et al.* 2020, Diana *et al.* 2019).

The studied building was instrumented during its demolition via 10 triaxial MEMS accelerometers (ADXL 354), placed in identical positions at levels 1 and 2 (as defined in Fig. 1(b)), at the positions marked in Fig. 1(c). Each triaxial sensor node was aligned with the longitudinal and transverse directions of the building, measuring horizontal accelerations along the two main axes Y and Z, as defined in Fig. 1(c). Typical sensor placement is depicted in Fig. 1(d). The data acquisition was conducted by means of a National Instruments cDAQ-9188 at a sampling rate of 1720 Hz. Weather conditions (cloudy at 15°C) were stable throughout the (relatively short) duration of measurements and thus, environmental conditions are considered not to alter material properties.

2.2 Demolition of masonry buildings

The demolition of masonry buildings is performed by gradual removal of structural elements from top to bottom with the shovel of an excavator. Non-structural elements,

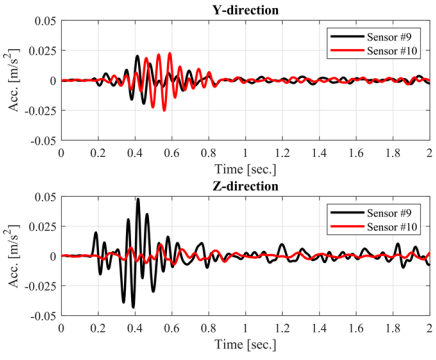

(a) Time-series of a characteristic shock

(b) Location of shovel-impact

Fig. 2 Shovel-hits on the undamaged building

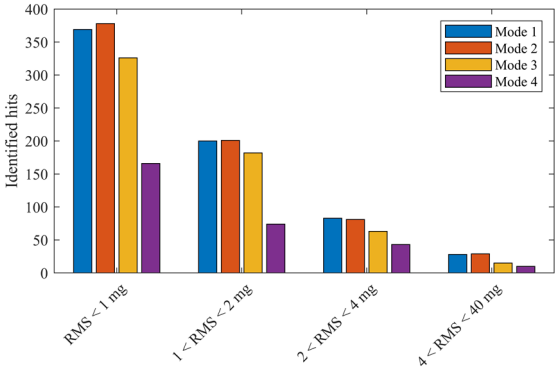

(a) Classification of detected impulses to amplitude bins

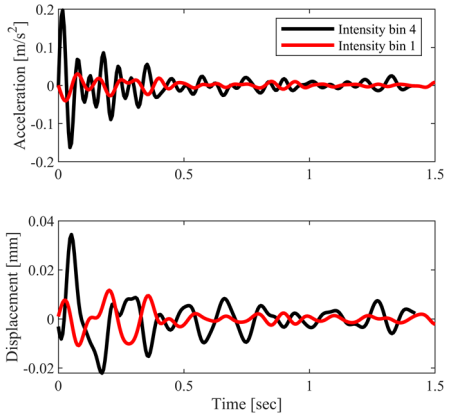

(b) Impulse response of sensor 9 (level 2, demolition side) for two amplitude levels

Fig. 3 Impulse classification to amplitude bins and response in time domain

including furniture, opening frames, glass windows, floor covering and roof tiling are extracted beforehand, leaving the structure at a bare state. This facilitates the inspection of structural materials and geometry. Such non-structural elements have been shown in the past to bear minor influence on the dynamic response of existing masonry buildings (Reuland *et al*. 2017b).

During demolition, buildings are subjected to hits and pulls of arbitrary direction and intensity, resulting in a rich variety of impulse responses. Fig. 2 contains an example of a hit with the excavator shovel. The resulting acceleration time series (Fig. 2(a)) indicate higher response amplitude along the transverse direction, which coincides with the direction of the hit. The amplitude is stronger in the vicinity of sensor 9, which is placed closer to the impact location. In the longitudinal direction (axis Y), the time-delay of the impact between sensor 9 and sensor 10 is evident. Additionally, sensor 10, for which the Y-component of the acceleration is oriented along the out-of-wall plane, exhibits higher acceleration in this direction than the sensor closest to the impact, indicating the possible absence of diaphragmatic behavior of the floor slabs for higher amplitudes of excitation.

Although excitation amplitude, location and direction cannot be measured directly, the intensity metrics of the building response can be utilized to cluster the response impulses into groups of similar amplitude. To this end, the peak and root mean square (RMS) acceleration response during each impulse has been extracted and analyzed. For the demolition case analyzed in this paper, the recorded impulses are clustered into four amplitude-based bins, as demonstrated in Fig. 3(a). A total of 689 impulses have been recorded during the first 90 minutes of the demolition, when the works were limited to disassembling the roof and no structural damage beneath level 2 was observed. The range of the response amplitude in terms of RMS acceleration during each impulse varies between 0 and 0.04 g, up to 2 orders of magnitude higher than ambient vibrations. However, most of the identified impulses caused low levels of excitation (below 1 mg).

The signal measured by sensor 9, placed at level 2 on the demolition side (see Fig. 1(c)), is illustrated in Fig. 3(b) under hits of varying excitation level. The displacement response is derived through double integration of the acceleration signal, following the removal of linear trends through high-pass filtering with a cutoff frequency equal to 1 Hz. Since the characteristic frequencies of the structure lay above 5 Hz and the studied response does not include structural damage, the distortion of the signal due to high-pass filtering is considered minimal. Although the calculation of displacements based on numerical integration of acceleration recordings is not precise, it can be used to provide an estimate for the order of magnitude reached by the total displacement. As the maximum computed displacement is lower than 0.05 mm and the equivalent linear range, according to subsequent analysis (Section 4.3), covers the displacement range up to 1 mm, it can be assumed that the structure responds in the elastic range during demolition and no damage due to excessive loading is expected.

2.3 Model updating based on dynamic measurements during demolition

The workflow that is proposed for the inverse task of updating a finite-element (FE) model based on identified modal properties at different response amplitudes is illustrated in Fig. 4. Initially, a baseline identification on ambient recordings, prior to the beginning of any demolition activity, is conducted. This baseline identification provides estimates of the modal characteristics that are used for discarding erroneous identification results during demolition.

The signals recorded during the demolition are segmented into separate impulse responses that are further analyzed in the time domain with the Eigensystem Realization Algorithm (ERA) (Juang and Pappa 1985, Peterson 1995), which provides identification of modal properties (frequency, mode shape and damping) for each impulse response. In order to account for the effect of Hankel matrix truncation, each impulse response is analyzed multiple times following a grid sampling of possible values for the Hankel matrix length. The identified modal properties are considered valid if the corresponding

mode complies with three criteria: (i) mode-shape correspondence with the baseline modal identification is ensured by modal assurance criterion (MAC) (Allemang 2003) values over 80%; (ii) frequency fit, as defined by the compliance criterion of Eq. (1), with the baseline identification results should exceed a minimum threshold, set equal to 80%; and (iii) the Pearson's correlation coefficient between ERA prediction and the original measured response is constrained to exceed a threshold, which is also set to 80%.

$$CC_i^j = 0.5 \cdot \left[1 - \frac{\left|f_i^j - f_i^{ref}\right|}{f_i^{ref}}\right] + 0.5 \cdot MAC(\varphi_i^{ref}, \varphi_i^j) \quad (1)$$

In Eq. (1), f_i^{ref} and f_i^j represent the identified frequency of mode i from baseline identification and hit j respectively. In a similar manner, the Modal Assurance Criterion $MAC(\varphi_i^{ref}, \varphi_i^j)$ compares the i^{th} modal vector from the baseline identification procedure against the one extracted from hit j.

The definition of these tests and their corresponding thresholds is essential and needs to balance two competing goals: exclude erroneous identification results, which would artificially increase the uncertainty in identified modal properties, and include with high probability the changes in modal properties that originate from increasing amplitudes of excitation. The first two criteria compare the ERA identification results with the reference model and thus, increasing the thresholds could potentially exclude information related to phenomena that cannot be captured by the baseline identification on ambient excitation data. Additionally, targeting too high correlation between ERA predictions and measurements could lead to overfitting, due to short duration of the impulses and inherent noise of the recorded signals with low-cost sensors. The recommended range for these thresholds is set in this work between 70 % and 90%. A sensitivity analysis within this range showed no significant influence on either the overall performance of the algorithm or the identification results.

A parametric finite element model (FEM) of the studied structure is developed and proper ranges for the uncertain parameters, pertaining to material properties, boundary conditions and mass, are defined. The accepted identification results are clustered based on response amplitude metrics such as peak acceleration and RMS acceleration during the impulse (Fig. 3(a)). For each intensity bin, the uncertain parameters of the FEM are inferred using Bayesian model updating. The updated models can be used for the nonlinear seismic assessment, considering the code provisions and safety factors.

3. System Identification at Healthy State

Despite remaining in a healthy (undamaged) state for their entire service life, many buildings exhibit elastic (reversible) nonlinear behavior for dynamic excitation levels that exceed ambient shaking (Astorga *et al.* 2018). Masonry is an orthotropic and heterogeneous construction material and, as a consequence, masonry buildings are

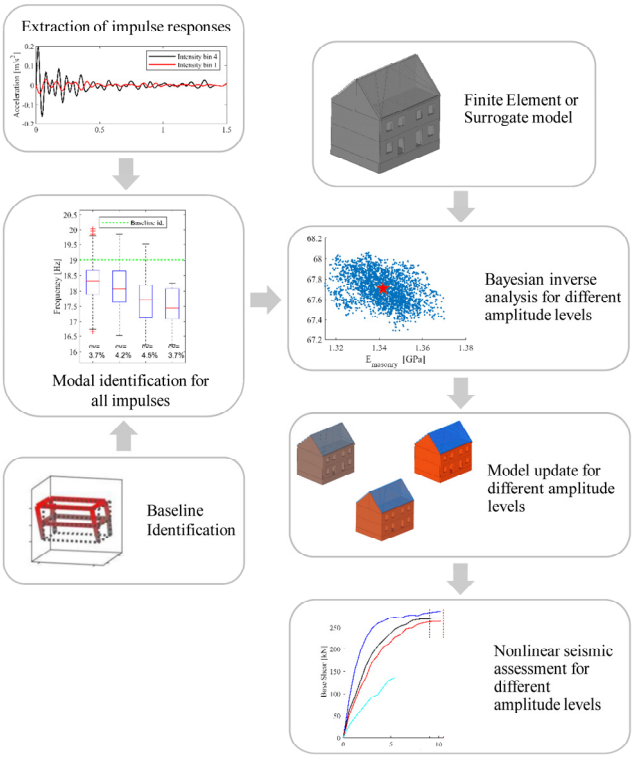

Fig. 4 Proposed framework for the inverse update and seismic evaluation of models for various response amplitude levels

prone to an even more prominent influence of the excitation amplitude on the structural response. Therefore, in this section, modal identification of a same building (see Fig. 1) is performed under ambient vibrations with classical output-only modal identification techniques and subsequently, modal properties are also derived for excitations originating from demolition activities. Such excitations exceed the level of typical ambient-vibration levels. It is highlighted that the present work focuses exclusively on the response during the first 90 minutes of the deconstruction process, before the demolition reached structural parts. Therefore, the observed nonlinearities, which are amplitude dependent, are not related to permanent structural damage and the structure is considered to remain in healthy state; especially as the changes in dynamic properties are reversible.

3.1 Baseline identification

A baseline identification of the modal characteristics, considering ambient recordings before the beginning of the demolition, is conducted by implementing the Stochastic Subspace Identification algorithm (Van Overschee and De Moor 1996) for the given sensor configuration (Fig. 1(c)). A standard pre-processing has been conducted, consisting of bandpass filtering between 1 and 40 Hz, exclusion of linear trends and down-sampling from 1720 to 172 Hz. The identified modal characteristics of the first four stable modes are summarized in Fig. 5. The characteristic frequencies of the structure are found to lie between 6 and 20 Hz. The first two modal shapes correspond to the main translational degrees of freedom of the building (first mode

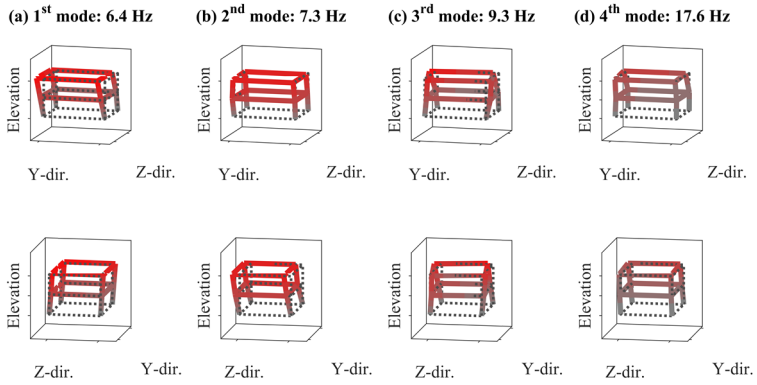

Fig. 5 Overview of the identified modal characteristics based on measurements under ambient vibrations prior to demolition. Each column demonstrates the corresponding modal shape from different viewpoints

in the longer direction, Y, and second mode in the shorter direction, Z, as defined in Fig. 1). The third modal shape seems associated with a torsional mode and the fourth modal shape includes a combination of rotational and translational degrees of freedom. It is mentioned that the building is softer in the longitudinal direction (axis Y), which is attributed to the large openings of the corresponding facades (Fig. 1(c)). This baseline identification serves as reference for the subsequent time-domain analysis (as described in Section 2.3) at the beginning of the deconstruction process, before any visible structural damage to the first two floors occurred. Due to the use of low-cost MEMS accelerometers on such a stiff low-rise building, modal identification is typically limited to few modes of vibration.

3.2 Operational modal analysis during demolition

During demolition, the response amplitude exceeds typical levels of ambient vibrations, even before the structure sustains observable damage or permanent changes in stiffness and mass. Although it is impossible to quantify the input directly, response impulses of various amplitudes are utilized to identify the modal characteristics at different amplitude levels. Typical impulse responses for different amplitude levels are shown in Fig. 3(b).

The effect of strong hits with the excavator shovel on the modal properties is studied in detail in Fig. 6. The first impulse corresponds to the acceleration response history plotted in Fig. 2(a). The frequency-domain characteristics are derived through application of the Frequency-Domain-Decomposition method (Brincker *et al*. 2001) over a time-window of 1.5 s and with a frequency resolution of 0.1 Hz. In order to increase the frequency-domain resolution, zero-padding is applied. The frequency-domain characteristics are calculated for a sliding window with a time increment of 0.01 sec.

Fig. 6(b) contains the first singular value of the spectral densities, providing an indication of the energy spread within the frequency domain. The hits are more prominent in the higher frequencies, as the fourth mode (at 17.6 Hz) shows the highest spectral density for the first hit, while the third mode (at 9.3 Hz) contains most energy for the second hit. The spectral-energy content, together with the duration of high-amplitude vibrations, present the highest discrepancy between vibrations created by shovel impacts and earthquake excitation, as for the latter case, fundamental modes carry more energy. Nevertheless, data recorded under impulse-like excitation during demolition processes are deemed representative of changes in overall dynamic behavior due to changes in response amplitude.

In Fig. 6(c), the evolution of the frequency values, compatible with the first translational mode (along the Y-axis), is traced over time. As the excitation is not symmetric, only the Y-components of the measurements are used to compare the modal shapes. Prior to the hit, as vibrations remain at low amplitude levels, the compatible frequency values are densely grouped around the corresponding baseline identification frequency (indicated by a dotted green line). The highest spectral energy points are indicated with red dots, forming point estimates for the evolution of the corresponding frequency value. Finally, the red-dotted boxes enclose the time-window of the first hit, which contains mostly Z-direction components. A short-term reduction in frequency during higher-amplitude excitation can be observed in Fig. 6(c). A similar - even more pronounced - behavior can be observed for the second mode (Fig. 6(d)), which corresponds to translation along Z-direction. As evidenced by the evolution of the first two natural frequencies, higher amplitudes of excitation lead to a short-time drop in the estimated frequency, before returning to a level that is similar to the pre-hit level.

Fig. 6(e) shows the evolution of the frequency values for which the modal displacements are compatible with the third/rotational mode (Fig. 5(c)). As the hits do not provide similar excitation in both directions, no compatible mode-shape can be found during the first hit (red-dotted box). However, a reduction in frequency after the hit is evident. The effect of a singular hit on the frequency exposes the short-term influence of response amplitude on modal properties. In order to highlight the systematic influence of vibration amplitude on the global dynamic response, a statistical approach, as described in section 3.2, is required. As the hits can be assimilated to impulse-like responses, the ERA method is used to derive the natural frequencies, the equivalent viscous damping and the modal displacements for each detected hit. The influence of response amplitude on the identified natural frequencies of the first four global

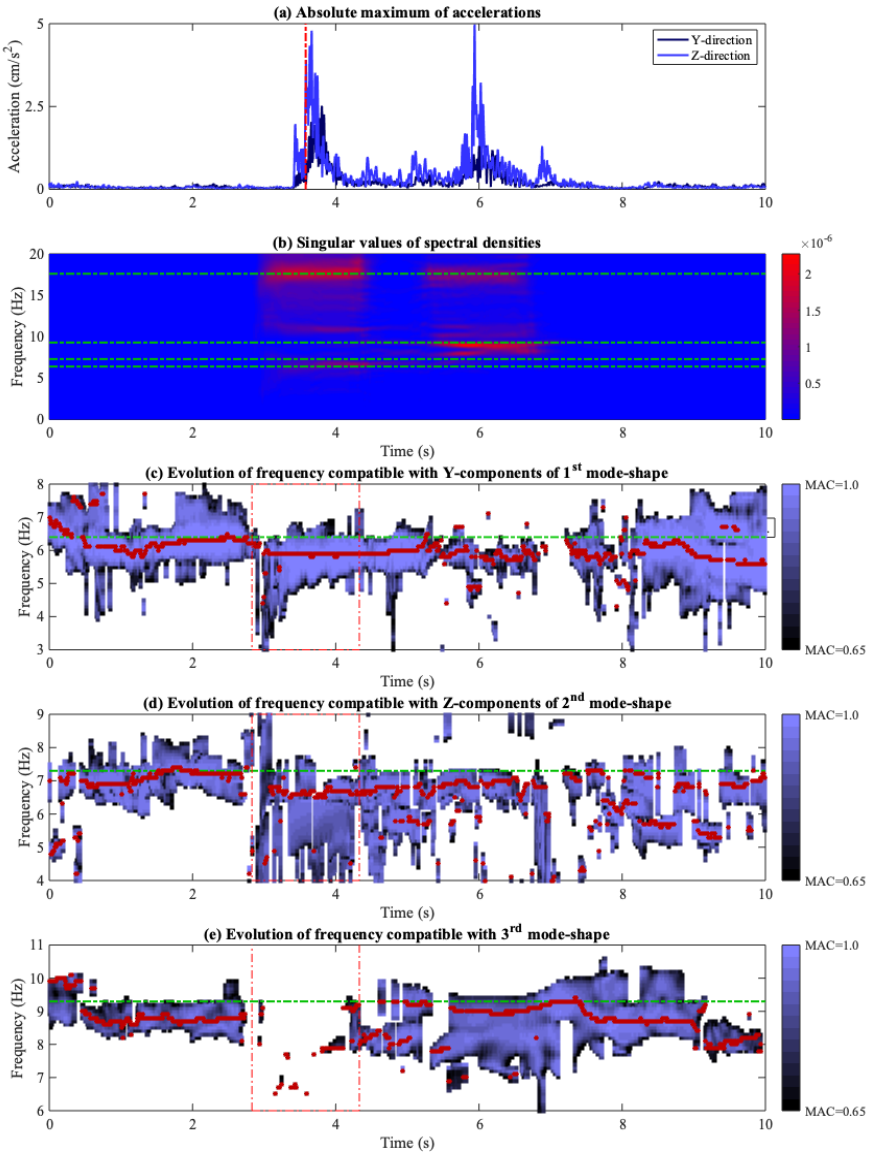

Fig. 6 Frequency evolution in the time-domain under two consecutive strong hits

vibration modes is shown in Fig. 7, together with the corresponding baseline identification, based on ambient recordings.

Due to the short duration of the impulses, their arbitrary input (location, direction and amplitude) and the inherent measurement noise, the operational modal analysis procedure is only able to identify the excited modes during the studied impulse, that in certain cases include transient local phenomena. In order to ensure consistency of the identified modal properties and to limit identification to the global modal shapes, three criteria for modal identification are implemented. As described in Section 2.3, these criteria involve the baseline identification results and the goodness of fit between ERA predictions and real response. All detected hits during the first 90 minutes of the deconstruction process (before the demolition reached structural parts of the two main floors) are clustered into groups of similar response amplitudes (see Fig. 3(a)). It is noted that the changes in modal parameters are reversible and thus, can be attributed to the response amplitude and not to potential minor changes to the building introduced by demolition activity. Most impulses correspond to low amplitude levels, with RMS acceleration below 1 mg. The first three modes are detected in the majority of the impulses, while the 4th mode is identified in nearly 40% of the hits.

The descriptive statistics of the identified natural frequencies, as well as the point estimations of the baseline identification are summarized in the boxplots of Fig. 7. The baseline identification tends to overestimate the frequency, as it lays above the 75th percentile for the modes 1, 3 and 4. This shows that even for small-amplitude hits, the dynamic response of the building demonstrates a softening behavior. For the first two modes, the reduction of median frequency between the first and the fourth amplitude bin is respectively 5% and 7%. Given the approximate value of inter-storey drifts of 0.5-1 10^{-5}, these values of reduction in stiffness are in line with previous studies (Michel *et al.* 2011). The variability of the observed frequency remains mostly constant in relative terms (coefficient of variation

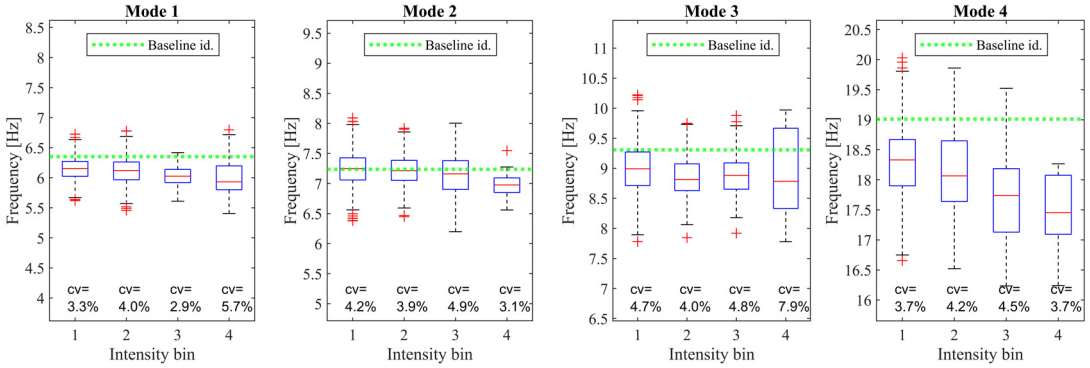

Fig. 7 Frequency evolution with increasing response amplitude. The red line indicates the median, while the blue box marks the first and third quartile and thus, contains 50% of the identified values. The whiskers indicate ± 2.7σ limits, over which the data are discarded as outliers

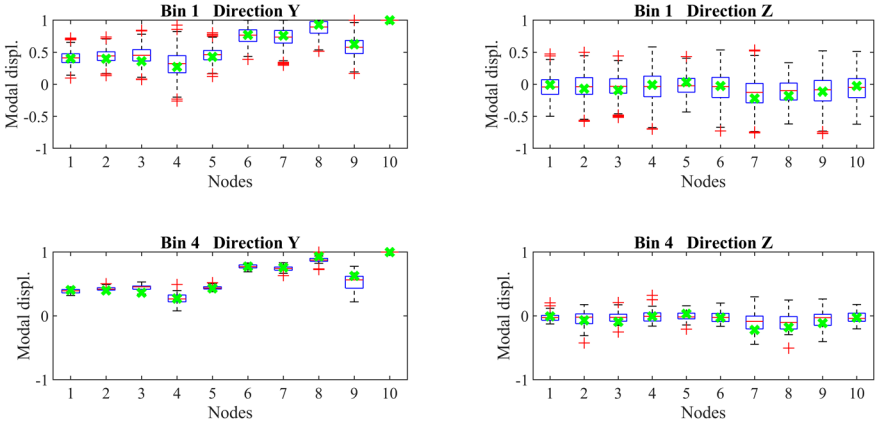

Fig. 8 Identified modal displacements for the first mode, for different amplitude bins. The direction refers to the axes defined in Fig. 1. The baseline identification is denoted via green crosses. The red line indicates the median, while the blue box marks the first and third quartile and thus, contains 50% of the identified values. The whiskers indicate ± 2.7σ limits, over which the data are discarded as outliers

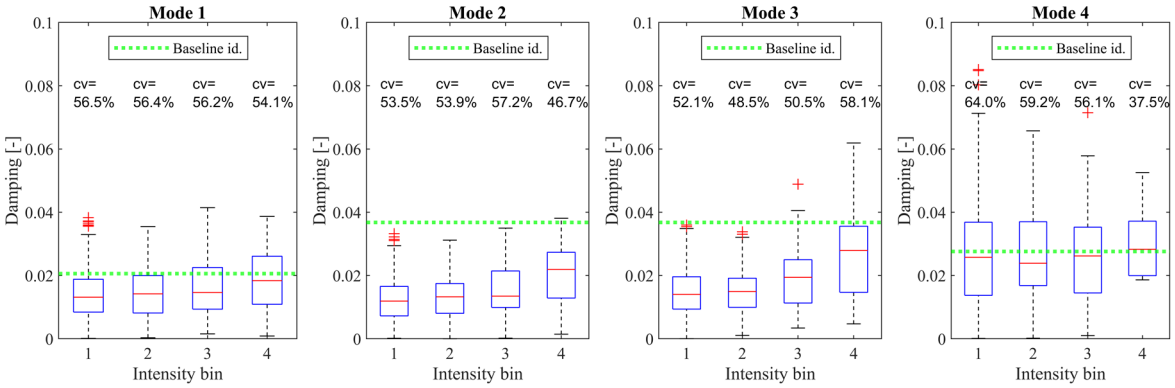

Fig. 9 Damping evolution with increasing response amplitude. The red line indicates the median, while the blue box marks the first and third quartile and thus, contains 50% of the identified values. The whiskers indicate ± 2.7σ limits, over which the data are discarded as outliers

below 0.05 for most cases), with a decrease for high amplitudes for the second mode and an increase in variability for the third mode. The increase in variability for the torsional mode can possibly be linked to the uni-directional nature of hits.

The identified modal displacements for the first mode are reported in Fig. 8, together with the point estimates of the baseline identification. As expected, the displacement coordinates of the first five nodes are lower, as they are placed at the first level of the building (Fig. 1). In general, the uncertainty of modal displacements reduces with increasing amplitude, which is consistent for all four identified modes. Node 9, placed at the second level of the building, yields lower modal displacements and higher

uncertainty compared to the other nodes placed at the same level. This behavior, which is not observed in higher modes, is attributed to the position of the sensor, adjacent to the demolition works, and to the missing diaphragm. The baseline identification seems to fit adequately the modal displacements for the first mode. Although, for higher modes, the reference identification lies outside the first or third quartile for certain nodes, indicating the limitations of point estimates against the statistical approach applied.

The reduction in frequency is accompanied by an increase in damping, as shown in Fig. 9. As expected, damping estimates have a large uncertainty and the values derived from ambient vibrations give unrealistic estimates for real damping under impulse loading. The damping estimates for the first three modes are similar, with median values around 1.5% for low-amplitude hits and roughly 2% for hits with higher amplitudes. This increase in damping may be explained by energy absorption from non-linear behavior due to opening and closure of micro-cracks or due to hysteretic behavior of soil, which is shown to exist even for very low strains, in the theoretical linear elastic regime (Martakis *et al*. 2017). Nevertheless, further studies would be necessary to explore energy dissipation at relatively low vibration amplitudes. Damping-ratio values are in agreement with previous work on masonry buildings (De Sortis *et al*. 2005). Also, values fall in between typical code-assumptions for damping (5%), which form an upper bound (including also hysteretic energy absorption) and damping ratios observed for shake table tests (below 1% as reported by Kouris *et al*. (2017), which can be considered a lower bound, due to absence of foundations and non-structural elements.

4. Structural model and data-driven parameter updating

The scope of this section is to shed light on the impact of conventional assumptions regarding highly uncertain model properties on the dynamic response predictions of existing masonry buildings and explore the benefit of dynamic measurements on the reduction of these uncertainties and finally on the outcome of seismic evaluations. The simplified model, which is used to predict modal properties, belongs to the category of equivalent-frame models.

4.1 Model description

Equivalent-frame models, with plasticity lumped into zero-length springs, are widely used for nonlinear design and assessment of existing masonry buildings. Despite the strong underlying assumptions, this method is popular, due to its simple modeling principles, the intuitive representation of the structural skeleton, the transparent consideration of a limited number of uncertain parameters and the successful capture of the structural response in the nonlinear regime (Belmouden and Lestuzzi 2009, Lagomarsino *et al*. 2013, Bracchi *et al*. 2015, Quagliarini *et al*. 2017). However, such models fail to represent all possible failure scenarios of masonry buildings, such as out-of-plane failure or bi-directional bending.

The studied structure is modelled using the commercial structural analysis software SAP2000, version 22 (CSI 2020), as a three-dimensional equivalent frame model (see Fig. 10 for the modelling assumptions). The structural walls are discretized into piers and spandrels with cross sections dictated by the real dimensions of the structure. The walls in the basement are considered elastic above and rigid beneath the ground level horizon. The foundation impedance is simulated with three translational and three rotational springs, that are placed at the geometrical center of the foundation, according to the analytical formulations proposed by Gazetas (1992). These formulations have been validated experimentally through statically imposed loads (Dobry *et al.* 1986), as well as through dynamic experiments in centrifuge, under realistic stress soil conditions (Martakis *et al*. 2017).

Uncertain parameters pertaining to material properties, boundary conditions and mass are considered random

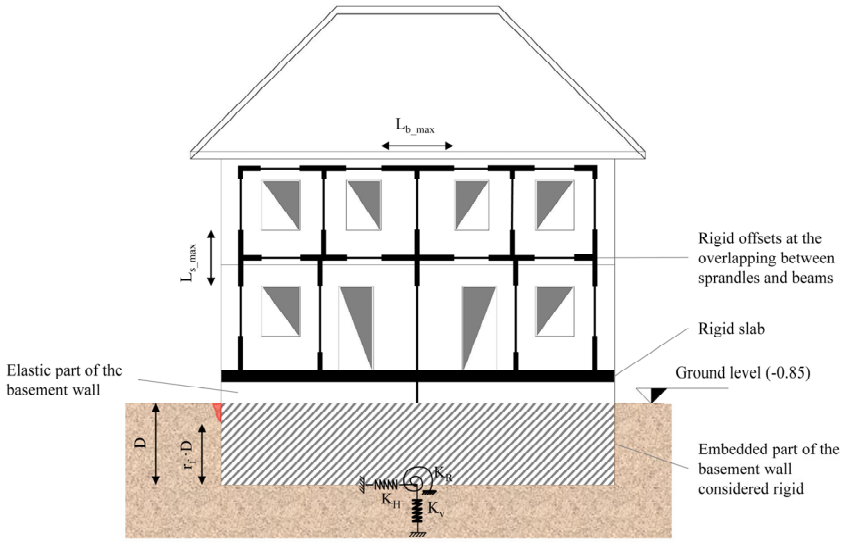

Fig. 10 Schematic representation of the finite-element implementation of the equivalent-frame model

variables with uniform distributions in predefined ranges that are chosen according to Swiss building codes (SIA 261, SIA 266, SIA 269/6 and SIA 269/8) and engineering judgment. The uncertain parameters and the corresponding ranges are summarized in Table 1. For the walls, apart from the modulus of elasticity and the unit weight, the overlapping between spandrels and piers, which defines rigid regions, are considered uncertain. The length of the rigid regions ranges from 30% to 100% of the maximum overlapping length (see Fig. 10). The timber beams of the slabs are aligned parallel to the short direction of the building (Z-direction in Fig. 1), which results in an orthotropic behavior. In order to account for the stiffness and mass distribution of timber floors, equivalent orthotropic slabs with constant thickness of 20 cm are adopted. The ranges for the elastic properties and unit weight are calculated in accordance to the timber floor dimensions (square beams with 25 × 25 cm section at a distance of 70 cm). The equivalent elastic properties and unit weight of the soil are considered very uncertain and thus, wide prior parameter ranges comprising all possible soil compositions, are defined according to Studer *et al*. (2007). Finally, the effective foundation embedment, accounting for loose contact with soil, according to Gazetas (1992), is bounded between 30% and 100% of the total embedment D, as schematized in Fig. 10.

4.2 Bayesian model updating

In order to determine the model parameters that best fit the identified modal properties, a Bayesian inference framework (Beck and Katafygiotis 1998) is implemented through the UQLab toolbox (Marelli and Sudret 2014, Wagner *et al*. 2019). In this framework, uncertain model parameters are considered as random variables with uniform prior distributions, per Table 1. These prior distributions are updated using measurement data, so that the posterior distributions combine the prior information and the information extracted from the modal identification data (frequencies of the first two modes and the corresponding modal displacements).

The computation of the posterior distributions is achieved via Markov-Chain Monte-Carlo sampling (Gelman *et. al*. 2014), by considering 10 Markov chains with 10'000 samples. In order to reduce the computational burden, a surrogate Polynomial Chaos Expansion model trained on 2000 runs of the original FEM was constructed and implemented in the MCMC simulation. The leave-one-out error between the surrogate model and the FEM model is calculated to be lower than 10^{-4} for the identified frequencies and lower than 0.025 for the identified modal shapes (normalized to the maximum modal displacement). This discrepancy is deemed acceptable compared to other sources of uncertainty. The computational model (M) provides response predictions ($\boldsymbol{y}$) for a given set of input parameters ($\boldsymbol{x}$). To account for measurement errors and model inaccuracy, a discrepancy term (ε) is considered, as a Gaussian random variable with zero mean and diagonal covariance matrix with constant variance equal to 0.0025

$$\boldsymbol{y} = M(\boldsymbol{x}) + \varepsilon \qquad \varepsilon \sim N(\varepsilon|0, \Sigma) \tag{2}$$

Consequently, all identified modal properties (characteristic frequencies and modal displacements) included in the output vector $\boldsymbol{y_i}$ for the i measurement are considered as equally weighted realizations of independent Gaussian distributions with mean values estimated from $M(\boldsymbol{x})$ and covariance matrix Σ. For N independent identification results (measurements, $\boldsymbol{Y} = \{\boldsymbol{y_i}, \ldots, \boldsymbol{y_N}\}$) and M identified modal properties ($\boldsymbol{y_i} = \{y_{ij}, \ldots, y_{iM}\}$), the likelihood is estimated from the multivariate Gaussian distribution, which is formed as the product of the above marginal Gaussian distributions and can be written as

$$\mathcal{L}(\boldsymbol{x}, \boldsymbol{Y}) = \prod_{i=1}^{N} \prod_{j=1}^{M} N\left(y_{ij} | M(\boldsymbol{x}), \Sigma\right) \tag{3}$$

Uncertainties are a crucial aspect of model updating (Simoen *et al*. 2015, Reuland *et al*. 2017a). A-priori estimation of more precise uncertainty structures (bias and correlation) or identification of exact variance estimates (Song *et al*. 2019a) are outside the scope of this paper. In addition, selection of the optimal model-class for the problem at hand (Muto and Beck 2008, Reuland *et al*. 2019b) is not performed. Simplified models, such as the equivalent-frame model used here, fail to capture all the physics of real building responses. As the discrepancy

Table 1 Prior and posterior ranges for modeling parameters, based on the baseline identification. The posterior ranges of the parameters that are considered independent from the response amplitude are highlighted

	Walls				Foundation & Soil			
	E [GPa]	w [kN/m^3]	r_{pier} [%]	r_{spr} [%]	G [MPa]	v [-]	w [kN/m^3]	r_{found} [%]
Prior	0.6-3	15-18	30-100	30-100	50-100	0.15-0.45	14-19	30-100
Post.	1.41-1.66	15-15.8	91-100	37-60	65-69	0.19-0.28	18.7-19	30-40

	Equivalent slabs (t = 20 cm)			
	$E_{//}$ [GPa]	$E_{\perp}$ [GPa]	w [kN/m^3]	Top ceiling load [kN/m^2]
Prior	1-5	1-2	1-3	1-3
Post.	2.23-4.22	1.51-1.59	2.1-3	2.7-3

between equivalent-frame models and real behavior is smallest for the fundamental translational modes, only the first two modes are used for Bayesian model updating. In addition, the assumption of zero-mean uncorrelated uncertainties does not compromise the purposes of this analysis, which focuses on the comparison of the inferred model parameters for different response amplitude levels, rather than exact predictions for risk-based decision making.

For the Bayesian model updating, the displacements and frequencies of the first two modes that correspond to the translational modal shapes of the structure are considered. Higher modes include rotational movements that are poorly captured by equivalent frame models, while they typically have lower modal mass and thus, have a reduced influence on the seismic assessment through nonlinear pushover analysis (Penelis 2006, Marino *et al*. 2019).

Starting from the uniform distributions defined in Table 1, the affine-invariant ensemble sampler (Goodman and Weare 2010) is implemented, in order to generate sufficient samples from the posterior distributions of the uncertain parameters. Initially, the baseline identification results (obtained for ambient vibrations) are used to infer parameter values that are independent from excitation amplitude. The posterior ranges are very narrow, providing precise point estimates of unit weights, top ceiling load and Poisson's ratio of the soil. These parameter values are considered constant for the subsequent analysis, as they are not expected to vary with increasing intensity. The prior and posterior distributions of all uncertain parameters pertaining to baseline identification are reported in Table 1.

In order to highlight the effect of response amplitude on the inferred stiffness properties, the Bayesian inverse analysis is conducted for each amplitude-related bin defined in Fig. 3(a). The posterior distributions of the inferred stiffness properties are sampled via the affine-invariant ensemble sampler (Goodman and Weare 2010) applied on the identified modal properties corresponding to each bin. The posterior distributions of the equivalent elastic modulus of masonry and the G-modulus of the soil for the amplitude bin 4 (highest amplitudes) are illustrated in Fig. 11. It can be observed that the posterior ranges are very narrow and thus, the mean value is considered as an adequate point estimate. The mean point estimates of all uncertain parameters for all amplitude-bins are summarized in Table 2.

As discussed in Section 3.3, the identified modal frequencies tend to drop with increasing response amplitudes, indicating nonlinear behavior in the equivalent elastic range of the response, before any damage occurs. To this end, the results from Bayesian model updating for increasing response amplitudes provide valuable insights into the properties that cause these shifts. As stated in previous work of the authors (Martakis *et al*. 2017), inertial

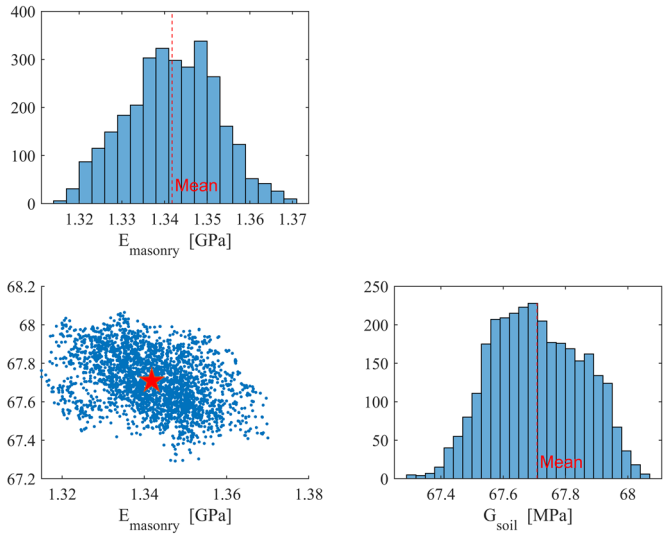

Fig. 11 Posterior distribution and correlation of the equivalent elastic stiffness properties of masonry and the soil for intensity bin 4 (highest amplitudes). Prior distributions are [0.6, 2.0] GPa for E-modulus of masonry and [50, 100] MPa for the G-modulus of the soil

Table 2 Posterior mean point estimates of stiffness related parameters for increasing response amplitude

	Walls			Foundation & Soil		Equivalent slabs (t = 20 cm)	
Ampl. Bin	E [GPa]	r_{pier} [%]	r_{spr} [%]	G [MPa]	r_{found} [%]	$E_{//}$ [GPa]	$E_{\perp}$ [GPa]
1	1.64	95	31	67.8	30	1.6	1.0
2	1.64	97	30	66.1	30	1.0	1.0
3	1.65	96	32	67.4	33	1.2	1.0
4	1.34	97	31	67.7	30	1.2	1.1

soil-structure interaction effects cause transient shifts of the equivalent elastic properties of the system Structure-Foundation-Soil, even at very low amplitude, in the equivalent linear elastic regime. However, in this case study, the governing parameter for the system softening due to increasing response amplitudes is the elastic modulus of masonry. The comparison of the inferred values of elastic modulus for increasing amplitude exposes a stiffness reduction of 18% between amplitude bins 1 and 4 (Fig. 12). The corresponding shift of the predicted frequencies is significantly lower (below 5%) and less evident, as no clear decreasing tendency can be justified between bins 1 and 4. Hence, Bayesian model updating, based on identified modal properties, provides robust estimates of the equivalent elastic properties that are sensitive to changes in stiffness, due to increasing response amplitude.

4.3 Impact of parameter updating on seismic assessment

Knowledge of the influence of the amplitude of shaking on the assumed stiffness of masonry can find several practical applications, such as reducing the probability of false positives in automatic data-driven damage-detection schemes. Moreover, a better understanding of the amplitude-dependent stiffness of masonry buildings may enable a more refined prediction of the seismic displacement demand, especially under use of simplified static nonlinear methods, such as the N2-method proposed by Fajfar and Gašperšič (1996). Since regional risk assessment models widely rely on bi-linearized capacity curves, for which assumptions regarding reduced stiffness are taken, these would also profit from monitoring-driven knowledge of amplitude-dependent stiffness drops.

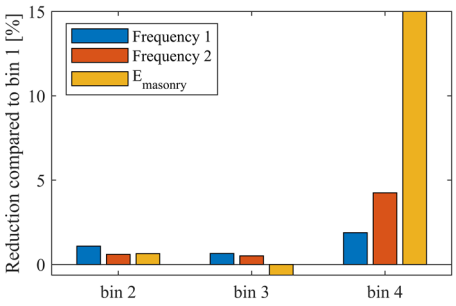

Fig. 12 Shifts in frequency predictions and changes in the inferred values of the E-modulus of masonry for increasing amplitude, considering amplitude-bin 1 as reference

In this section, an equivalent-frame model, based on the Tremuri method (Lagomarsino *et al*. 2013), is used to perform a static nonlinear seismic assessment (Fig. 13(a)). Although simplified, such a model helps in investigating the effect of updated elastic-parameter values on the seismic assessment. Given that the openings are essentially placed in the longitudinal direction (Y-direction in Fig. 1), pushover results are shown only for this direction, as the building strength is considered sufficient in the transversal direction. Piers and spandrels correspond to the scheme shown in Fig. 10. The seismic assessment is done using the basic assumptions prescribed by Swiss building codes (SIA 266, SIA 269/6 and SIA 269/8) and therefore, the compressive strength of masonry is taken as 0.001 times the elastic modulus and the G-modulus as 0.4 times the elastic modulus. In addition, the building is considered to be rigidly anchored to the ground and the clamping horizon corresponds to the ground level in Fig. 10. Local collapse mechanisms (such as out-of-plane failure of walls) are not examined, as they do not belong to the scope of this analysis and are not captured by equivalent frame models.

The pushover curves, obtained via imposed displacements that are proportional to the first mode shape, are reported in Fig. 13(b). The spectral demand is calculated from the Swiss design spectrum for seismic zone 2 and soil class E (SIA 261). The ultimate displacement of the capacity curve is defined as failure of the first load-bearing element. As can be seen in Fig. 13(b), elastic parameters, namely the elastic modulus of masonry, have an important influence on the overall nonlinear capacity curve. In order to demonstrate the effect of the uncertainty in the elastic stiffness on the calculated seismic performance, the lower and upper bound for the elastic modulus, according to relevant literature and existing building standards (SIA269/8, OPCM3274), have been considered. The estimated safety factor varies between 0.3, with practically no ductility, and 1.7, with ductility over 3. These extreme

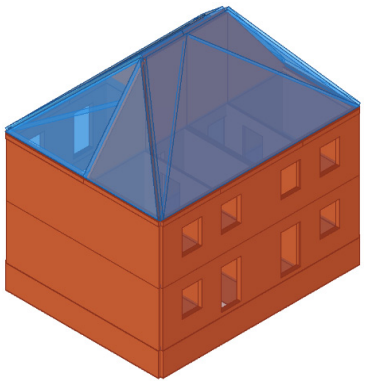

(a) 3D representation of the computational model. The clamped horizon is placed at the ground level

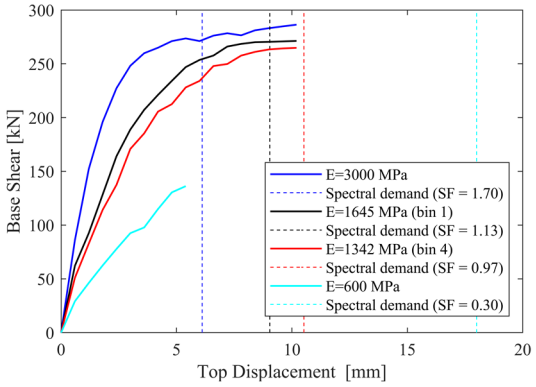

(b) Pushover curves, corresponding spectral demands and Safety Factors (SF) for varying E-modulus of masonry

Fig. 13 Effect of response amplitude on the seismic performance, estimated through nonlinear pushover analysis

cases expose the uncertainty pertaining to seismic assessment without prior information on the equivalent elastic stiffness. To this end, model updating is necessary in order to obtain robust estimates of the stiffness and reduce the uncertainty of the expected seismic performance.

When comparing the predictions resulting from model updating for bin 1 and 4, the E modulus drops by 18 % (see Section 4.2 and Table 2). This change in the elastic modulus translates to a reduction of the safety factor from 1.13 to 0.97. This significant reduction indicates the impact of stiffness changes at very-low amplitude excitation on global seismic performance. While the ultimate displacement and the maximum shear strength do not vary much, the reduction in stiffness increases the yield displacement and thus, reduces the post-yield displacement capacity. In addition, the displacement demand depends directly on the elastic branch of the equivalent bilinear capacity curve. Therefore, lower stiffness values (for an overall stiff building typology, such as the low-rise shear building under study) translate to higher displacement demands.

It has to be noted that both nominal and monitoring extracted values of the E-modulus are further reduced by 50% for the pushover analysis, to account for the cracked state of the material. The value of 50% can be considered to be arbitrary and the extent to which it covers stiffness changes under low amplitudes is debatable. Stronger hits and measurements under earthquake loads would be required to quantify the stiffness drop at the equivalent yield point.

Although the recorded hits produce displacements that are lower than 0.1 mm, corresponding to the very beginning of the predicted pushover curve (Figs. 3(b) and 13(b)), nonlinearities have been observed (Section 3.3) and found to cause significant stiffness-reduction (Section 4.2). Thus, the impulse responses generated during the demolition process expose nonlinearities in the commonly assumed linear elastic range. While the pushover analysis is highly simplified, and application to additional buildings is required to formalize the findings, it is concluded that systematic measurement of buildings that are being demolished can help in acquiring a better understanding of the dynamic properties, and by extension of the seismic safety, of existing structures.

5. Conclusions

The influence of changes in the amplitude of shaking on the dynamic properties of a masonry structure and as a result on its elastic parameters, obtained by updating a physics-based model, has been studied in this paper. Based on the presented monitoring campaign on a real masonry building, equipped with sensors during planned demolition, the following conclusions are drawn:

- Nonlinear behavior is observed in the elastic portion of the building response, without visible damage. Low-cost sensors can evidence such nonlinearity during demolition activities, which carries the potential for a systematic analysis of this behavior, particularly in countries with low-to-moderate seismicity. Nonlinearities can be tracked under one isolated hit, and by applying a statistical analysis of all possible hits and stronger vibrations that are created by demolition activities.
- Through updating a physics-based model, the changes in frequencies and modal shapes that are observed under increasing levels of shaking are shown to be related to changes in stiffness of the masonry, and not to transient changes in the foundation properties.
- Stiffness parameters, which are obtained through data-driven model updating, deliver a more sensitive indicator of changes in stiffness than modal frequencies.
- The stiffness reduction at low excitation levels, which is modelled to be linear in classical engineering assessment approaches, affects substantially the global seismic performance of the structure.

With the feasibility of such approaches verified in this first stage, future work is planned in order to systematically study the phenomenon on multiple buildings. By such an analysis, the influence of the building type on the sensitivity of modelling parameters to the response amplitude can be assessed and would be a valuable starting point for many applications in structural health monitoring. In addition, the necessary conditions for inclusion of higher modes into physics-based models will be investigated, with the goal to not compromise the computational burden of nonlinear seismic assessment.

Acknowledgments

The research described in this paper was financially supported by the Real-time Earthquake Risk Reduction for a Resilient Europe 'RISE' project, financed under the European Union's Horizon 2020 research and innovation programme, under grant agreement No. 821115, as well as the ETH Grant (ETH-11 18-1) Dynarisk - "Enabling Dynamic Earthquake Risk Assessment".

Authors would like to thank Kibag and Mr. Mario Sülz for granting access to the building during demolition, Professor Gramazio for providing valuable information regarding the examined building, Mr. Dominik Werne of the IBK Structures Lab for his valuable support in preparation of the monitoring equipment, and Mr. Martin Villanueva for his contribution to the equivalent-frame model.

References

Allemang, R.J. (2003), "The modal assurance criterion–twenty years of use and abuse", *Sound Vib*., **37**(8), 14-23.

Altunişik, A.C., Karahasan, O.Ş., Genç, A.F., Okur, F.Y., Günaydin, M. and Adanur, S. (2018), "Sensitivity-based model updating of building frames using modal test data", *KSCE J. Civil Eng.*, **22**(10), 4038-4046. https://doi.org/10.1007/s12205-018-1601-6

Asgarieh, E., Moaveni, B. and Stavridis, A. (2012), "Nonlinear structural identification of a three-story infilled frame using

instantaneous modal parameters", *Topics in Modal Analysis II*, **6**, 669-674. https://doi.org/10.1007/978-1-4614-2419-2_66

Astorga, A., Guéguen, P. and Kashima, T. (2018), "Nonlinear Elasticity Observed in Buildings during a Long Sequence of EarthquakesNonlinear Elasticity Observed in Buildings during a Long Sequence of Earthquakes", *Bull. Seismol. Soc. America*, **108**(3A), 1185-1198. https://doi.org/10.1785/0120170289

Atamturktur, S. and Laman, J.A. (2012), "Finite element model correlation and calibration of historic masonry monuments", *Struct. Des. Tall Special Build.*, **21**(2), 96-113. https://doi.org/10.1002/tal.577

Bakir, P.G., Reynders, E. and De Roeck, G. (2007), "Sensitivity-based finite element model updating using constrained optimization with a trust region algorithm", *J. Sound Vib.*, **305**(1-2), 211-225. https://doi.org/10.1016/j.jsv.2007.03.044

Bartoli, G., Betti, M., Facchini, L., Marra, A.M. and Monchetti, S. (2017), "Bayesian model updating of historic masonry towers through dynamic experimental data", *Procedia Eng.*, **199**, 1258-1263. https://doi.org/10.1016/j.proeng.2017.09.267

Beck, J.L. and Au, S.K. (2002), "Bayesian updating of structural models and reliability using Markov chain Monte Carlo simulation", *J. Eng. Mech.*, **128**(4), 380-391. https://doi.org/10.1061/(ASCE)0733-9399(2002)128:4(380)

Beck, J.L. and Katafygiotis, L.S. (1998), "Updating models and their uncertainties. I: Bayesian statistical framework", *J. Eng. Mech.*, **124**(4), 455-461. https://doi.org/10.1061/(ASCE)0733-9399(1998)124:4(455)

Bedon, C. (2019), "Diagnostic analysis and dynamic identification of a glass suspension footbridge via on-site vibration experiments and FE numerical modelling", *Compos. Struct.*, **216**, 366-378. https://doi.org/10.1016/j.compstruct.2019.03.005

Behmanesh, I., Moaveni, B. and Papadimitriou, C. (2017), "Probabilistic damage identification of a designed 9-story building using modal data in the presence of modeling errors", *Eng. Struct.*, **131**, 542-552. https://doi.org/10.1016/j.engstruct.2016.10.033

Belmouden, Y. and Lestuzzi, P. (2009), "An equivalent frame model for seismic analysis of masonry and reinforced concrete buildings", *Constr. Build. Mater.*, **23**(1), 40-53. https://doi.org/10.1016/j.conbuildmat.2007.10.023

Bracchi, S., Rota, M., Penna, A. and Magenes, G. (2015), "Consideration of modelling uncertainties in the seismic assessment of masonry buildings by equivalent-frame approach", *Bull. Earthq. Eng.*, **13**(11), 3423-3448. https://doi.org/10.1007/s10518-015-9760-z

Brincker, R., Zhang, L. and Andersen, P. (2001), "Modal identification of output-only systems using frequency domain decomposition", *Smart Mater. Struct.*, **10**(3), 441-445. https://doi.org/10.1088/0964-1726/10/3/303

Ceravolo, R., Matta, E., Quattrone, A. and Zanotti Fragonara, L. (2017), "Amplitude dependence of equivalent modal parameters in monitored buildings during earthquake swarms", *Earthq. Eng. Struct. Dyn.*, **46**(14), 2399-2417. https://doi.org/10.1002/eqe.2910

Chatzis, M., Chatzi, E. and Smyth, A.W. (2015), "An experimental validation of time domain system identification methods with fusion of heterogeneous data", *Earthq. Eng. Struct. Dyn.*, **44**(4), 523-547. https://doi.org/10.1002/eqe.2528

Cheng, L., Yang, J., Zheng, D., Li, B. and Ren, J. (2015), "The health monitoring method of concrete dams based on ambient vibration testing and kernel principle analysis", *Shock Vib.* https://doi.org/10.1155/2015/342358

Cheung, S.H. and Beck, J.L. (2009), "Bayesian model updating using hybrid Monte Carlo simulation with application to structural dynamic models with many uncertain parameters", *J. Eng. Mech.*, **135**(4), 243-255. https://doi.org/10.1061/(ASCE)0733-9399(2009)135:4(243)

Crowley, H., Despotaki, V., Rodrigues, D., Silva, V., Toma-Danila, D., Riga, E., Karatzetzou, A., Fotopoulou, S., Zugic, Z., Sousa, L. and Ozcebe, S. (2020), "Exposure model for European seismic risk assessment", *Earthq. Spectra.*, **36**(1), 252-273. https://doi.org/10.1177/8755293020919429

CSI (2020), SAP2000 Integrated Software for Structural Analysis and Design, Computers and Structures Inc., Berkeley, CA, USA.

De Sortis, A., Antonacci, E. and Vestroni, F. (2005), "Dynamic identification of a masonry building using forced vibration tests", *Eng. Struct.*, **27**(2), 155-165. https://doi.org/10.1016/j.engstruct.2004.08.012

Diana, L., Thiriot, J., Reuland, Y. and Lestuzzi, P. (2019), "Application of association rules to determine building typological classes for seismic damage predictions at regional scale: the case study of Basel", *Frontiers Built Environ.*, **5**. https://doi.org/10.3389/fbuil.2019.00051

Dobry, R., Gazetas, G. and Stokoe, K.H. (1986), "Dynamic response of arbitrarily shaped foundations: experimental verification", *J. Geotech. Eng.*, **112**(2), 136-154. https://doi.org/ 10.1061/(ASCE)0733-9410(1986)112:2(136)

Fajfar, P. and Gašperšič, P. (1996), "The N2 method for the seismic damage analysis of RC buildings", *Earthq. Eng. Struct. Dyn.*, **25**(1), 31-46. https://doi.org/10.1002/(SICI)1096-9845(199601)25:1<31::AID-EQE534>3.0.CO;2-V

Foti, D., Gattulli, V. and Potenza, F. (2014), "Output-only identification and model updating by dynamic testing in unfavorable conditions of a seismically damaged building", *Comput.-Aided Civil Infrastruct. Eng.*, **29**, 659-675. https://doi.org/10.1111/mice.12071

Gattulli, V., Antonacci, E. and Vestroni, F. (2013), "Field observations and failure analysis of the Basilica S. Maria di Collemaggio after the 2009 L'Aquila earthquake", *Eng. Fail. Anal.*, **34**, 715-134. http://dx.doi.org/10.1016/j.engfailanal.2013.01.020

Gazetas, G. (1992), "Formulas and charts for impedances of surface and embedded foundations", *J. Geotech. Eng.*, **117**(9), 1363-1381. https://doi.org/10.1061/(ASCE)0733-9410(1991)117:9(1363)

Gelman, A., Carlin, J.B., Stern, H.S., Dunson, D.B., Vehtari, A. and Rubin, D.B. (2014), *Bayesian Data Analysis*, Texts in Statistical Science, Boca Raton, FL, USA.

Goodman, J. and Weare, J. (2010), "Ensemble samplers with affine invariance", *Commun. Appl. Mathe. Computat. Sci.*, **5**(1), 65-80. https://doi.org/10.2140/camcos.2010.5.65

Jaishi, B. and Ren, W.X. (2005), "Structural finite element model updating using ambient vibration test results", *J. Struct. Eng.*, **131**(4), 617-628. https://doi.org/10.1061/(ASCE)0733-9445(2005)131:4(617)

Jensen, H.A., Millas, E., Kusanovic, D. and Papadimitriou, C. (2014), "Model-reduction techniques for Bayesian finite element model updating using dynamic response data", *Comput. Methods Appl. Mech. Eng.*, **279**, 301-324. http://dx.doi.org/10.1016/j.cma.2014.06.032

Juang, J.N. and Pappa, R.S. (1985), "An eigensystem realization algorithm for modal parameter identification and model reduction", *J. Guidance Control Dyn.*, **8**(5), 620-627. http://dx.doi.org/10.2514/3.20031

Kenny, C. (2009), "Why do people die in earthquakes? The costs, benefits and institutions of disaster risk reduction in developing countries", Research Report No. 4823, The World Bank Sustainable Development Network Finance Economics & Urban Department.

Kouris, L.A.S., Penna, A. and Magenes, G. (2017), "Seismic damage diagnosis of a masonry building using short-term damping measurements", *J. Sound Vib.*, **394**, 366-391. https://doi.org/10.1016/j.jsv.2017.02.001

Lagomarsino, S., Penna, A., Galasco, A. and Cattari, S. (2013), "TREMURI program: an equivalent frame model for the nonlinear seismic analysis of masonry buildings", *Eng. Struct.*, **56**, 1787-1799. http://dx.doi.org/10.1016/j.engstruct.2013.08.002

Lam, H.F., Hu, J. and Yang, J.H. (2017), "Bayesian operational modal analysis and Markov chain Monte Carlo-based model updating of a factory building", *Eng. Struct.*, **132**, 314-336. https://doi.org/10.1016/j.engstruct.2016.11.048

Lam, H.F., Hu, J. and Adeagbo, M.O. (2019), "Bayesian model updating of a 20-story office building utilizing operational modal analysis results", *Adv. Struct. Eng.*, **22**(16), 3385-3394. https://doi.org/10.1177%2F1369433218825043

Lombaert, G., Moaveni, B., He, X. and Conte, J.P. (2009), "Damage identification of a seven-story reinforced concrete shear wall building using Bayesian model updating", *Proceedings of the IMAC-XXVII*, Orlado, FL, USA, February.

Lourenço, P.B. and Roque, J.A. (2006), "Simplified indexes for the seismic vulnerability of ancient masonry buildings", *Constr. Build. Mater.*, **20**(4), 200-208. https://doi.org/10.1016/j.conbuildmat.2005.08.027

Ma, G. and Li, H. (2015), "Experimental study of the seismic behavior of predamaged reinforced-concrete columns retrofitted with basalt fiber–reinforced polymer", *J. Compos. Constr.*, **19**(6), 04015016. https://doi.org/10.1061/(ASCE)CC.1943-5614.0000572

Marino, S., Cattari, S. and Lagomarsino, S. (2019), "Are the nonlinear static procedures feasible for the seismic assessment of irregular existing masonry buildings?", *Eng. Struct.*, **200**, 109700. https://doi.org/10.1016/j.engstruct.2019.109700

Marelli, S. and Sudret, B. (2014), "UQLab: A framework for uncertainty quantification in Matlab", *Proceedings of the 2nd International Conference on Vulnerability*, *Risk Analysis and Management* (*ICVRAM2014*), Liverpool, UK.

Martakis, P., Taeseri, D., Chatzi, E. and Laue, J. (2017), "A centrifuge-based experimental verification of Soil-Structure Interaction effects", *Soil Dyn. Earthq. Eng.*, **103**, 1-14. https://doi.org/10.1016/j.soildyn.2017.09.005

Martakis, P., Dertimanis, V. and Chatzi, E. (2019), "Baudynamische Bemessung & Identifizierung einer Aufgehängten Treppenkonstruktion", *Proceedings of the 16th. D-A-CH Tagung Erdbebeningenieurwesen & Baudynamik* (*D-A-CH 2019*), Innsbruck, Austria.

Michel, C., Guéguen, P. and Bard, P.Y. (2008), "Dynamic parameters of structures extracted from ambient vibration measurements: An aid for the seismic vulnerability assessment of existing buildings in moderate seismic hazard regions", *Soil Dyn. Earthq. Eng.*, **28**(8), 593-604. https://doi.org/10.1016/j.soildyn.2007.10.002

Michel, C., Zapico, B., Lestuzzi, P., Molina, F.J. and Weber, F. (2011), "Quantification of fundamental frequency drop for unreinforced masonry buildings from dynamic tests", *Earthq. Eng. Struct. Dyn.*, **40**(11), 1283-1296. https://doi.org/10.1002/eqe.1088

Muto, M. and Beck, J.L. (2008), "Bayesian updating and model class selection for hysteretic structural models using stochastic simulation", *J. Vib. Control*, **14**(1-2), 7-34. https://doi.org/10.1177/1077546307079400

OPCM 3274 (2003), Primi elementi in materia di criteri generali per la classificazione sismica del territorio nazionale e di normative tecniche per le costruzioni in zona sismica.

Pai, S.G., Reuland, Y. and Smith, I.F.C. (2019), "Data-Interpretation Methodologies for Practical Asset-Management", *J. Sensor Actuator Networks*, **8**(2), 36. https://doi.org/10.3390/jsan8020036

Papadimitriou, C., Ntotsios, E., Giagopoulos, D. and Natsiavas, S. (2011), "Variability of updated finite element models and their predictions consistent with vibration measurements", *Struct. Control Health Monitor.*, **19**(5), 630-654. https://doi.org/10.1002/stc.453

Penelis, G.G. (2006), "An efficient approach for pushover analysis of unreinforced masonry (URM) structures", *J. Earthq. Eng.*, **10**(3), 359-379. https://doi.org/10.1080/13632460609350601

Peterson, L.D. (1995), "Efficient computation of the Eigensystem realization algorithm", *J. Guidance Control Dyn.*, **18**(3), 395-403. https://doi.org/10.2514/3.21401

Quagliarini, E., Maracchini, G. and Clementi, F. (2017), "Uses and limits of the Equivalent Frame Model on existing unreinforced masonry buildings for assessing their seismic risk: A review", *J. Build. Eng.*, **10**, 166-182. https://doi.org/10.1016/j.jobe.2017.03.004

Reuland, Y., Lestuzzi, P. and Smith, I.F. (2017a), "Data-interpretation methodologies for non-linear earthquake response predictions of damaged structures", *Frontiers Built Environ.*, **3**, 43. https://doi.org/10.3389/fbuil.2017.00043

Reuland, Y., Jaoude, A.A., Lestuzzi, P. and Smith, I.F. (2017b), "Usefulness of ambient-vibration measurements for seismic assessment of existing structures", *Proceedings of the 4th International Conference on Smart Monitoring*, *Assessment and Rehabilitation of Civil Structures*, Zurich, Switzerland.

Reuland, Y., Lestuzzi, P. and Smith, I.F.C. (2019a), "Measurement-based support for post-earthquake assessment of buildings", *Struct. Infrastruct. Eng.*, **15**(5), 647-662. https://doi.org/10.1080/15732479.2019.1569071

Reuland, Y., Lestuzzi, P. and Smith, I.F. (2019b), "An engineering approach to model-class selection for measurement-supported post-earthquake assessment", *Eng. Struct.*, **197**, 109408. https://doi.org/10.1016/j.engstruct.2019.109408

SIA 261 (2014), Einwirkungen auf Tragwerke, Swiss Society of Engineers and Architects: Zurich, Switzerland.

SIA 266 (2015), Mauerwerk, Swiss Society of Engineers and Architects: Zurich, Switzerland.

SIA 269/6 (2014), Erhaltung von Tragwerken - Mauerwerksbau, Teil 2: Mauerwerk aus künstlichen Steinen, Swiss Society of Engineers and Architects: Zurich, Switzerland.

SIA 269/8 (2017), Erhaltung von Tragwerken – Erdbeben, Swiss Society of Engineers and Architects: Zurich, Switzerland.

Simoen, E., De Roeck, G. and Lombaert, G. (2015), "Dealing with uncertainty in model updating for damage assessment: A review", *Mech. Syst. Signal Process.*, **56**, 123-149. https://doi.org/10.1016/j.ymssp.2014.11.001

Snoj, J., Österreicher, M. and Dolšek, M. (2013), "The importance of ambient and forced vibration measurements for the results of seismic performance assessment of buildings obtained by using a simplified non-linear procedure: case study of an old masonry building", *Bull. Earthqu. Eng.*, **11**, 2105-2132. https://doi.org/10.1007/s10518-013-9494-8

Song, M., Behmanesh, I., Moaveni, B. and Papadimitriou, C. (2019a), "Modeling error estimation and response prediction of a 10-story building model through a hierarchical Bayesian model updating framework", *Frontiers Built Environ.*, **5**. https://doi.org/10.3389/fbuil.2019.00007

Song, M., Moaveni, B., Papadimitriou, C. and Stavridis, A. (2019b), "Accounting for amplitude of excitation in model updating through a hierarchical Bayesian approach: Application to a two-story reinforced concrete building", *Mech. Syst. Signal Process.*, **123**, 68-83. https://doi.org/10.1016/j.ymssp.2018.12.049

Soyoz, S., Taciroglu, E., Orakcal, K., Nigbor, R., Skolnik, D., Lus, H. and Safak, E. (2013), "Ambient and forced vibration testing of a reinforced concrete building before and after its seismic retrofitting", *J. Struct. Eng.*, **139**(10), 1741-1752. http://dx.doi.org/10.1061/(ASCE)ST.1943-541X.0000568

Spencer, B.J., Finholt, T.A., Foster, I., Kesselman, C., Beldica, C.,

Futrelle, J., Gullapalli, S., Hubbard, P., Liming, L., Marcusiu, D., Pearlman, L., Severance, C. and Yang, G. (2004a), "NEESGRID: a distributed collaboratory for advanced earthquake engineering experiment and simulation", *Proceedings of the 13th World Conference on Earthquake Engineering*, Vancouver, B.C., Canada, August.

Spencer, B.J., Ruiz-Sandoval, M.E. and Kurata, N. (2004b), "Smart sensing technology: opportunities and challenges", *Struct. Control Health Monitor.*, **11**, 349-368. https://doi.org/10.1002/stc.48

Stavridis, A., Koutromanos, I. and Shing, P.B. (2011), "Shake-table tests of a three-story reinforced concrete frame with masonry infill walls", *Earthq. Eng. Struct. Dyn.*, **41**(6), 1089-1108. https://doi.org/10.1002/eqe.1174

Steiger, R., Feltrin, G., Weber, F., Nerbano, S. and Motavalli, M. (2015), "Experimental modal analysis of a multi-storey light-frame timber building", *Bull. Earthq. Eng.*, **15**(8), 3265-3291. https://doi.org/10.1007/s10518-015-9828-9

Straub, D. and Papaioannou, I. (2015), "Bayesian updating with structural reliability methods", *J. Eng. Mech.*, **141**(3), 04014134. https://doi.org/10.1061/(ASCE)EM.1943-7889.0000839

Studer, J.A., Laue, J. and Koller, M.G. (2007), *Bodendynamik*, Springer-Verlag Berlin, Heidelberg, Germany.

Tarantola, A. (2006), "Popper, Bayes and the inverse problem", *Nature Phys.*, **15**, 3265-3291. https://doi.org/10.1038/nphys375

Ulusoy, H.S., Feng, M.Q. and Fanning, P.J. (2010), "System identification of a building from multiple seismic records", *Earthq. Eng. Struct. Dyn.*, **40**, 661-674. https://doi.org/ 10.1002/eqe

Van Overschee, P. and De Moor, B. (1996), "Continuous-time frequency domain subspace system identification", *Signal Processing*, **52**(2), 179-194. https://doi.org/10.1016/0165-1684(96)00052-7

Vanik, M.W., Beck, J.L. and Au, S. (2000), "Bayesian probabilistic approach to structural health monitoring", *J. Eng. Mech.*, **126**(7), 738-745. https://doi.org/10.1061/(ASCE)0733-9399(2000)126:7(738)

Vidal, F., Navarro, M., Aranda, C. and Enomoto, T. (2014), "Changes in dynamic characteristics of Lorca RC buildings from pre-and post-earthquake ambient vibration data", *Bull. Earthq. Eng.*, **12**(5), 2095-2110. https://doi.org/10.1007/s10518-013-9489-5

Wagner, P.R., Nagel, J., Marelli, S. and Sudret, B. (2019), "UQLab user manual – Bayesian inference for model calibration and inverse problems", Report No. UQLab-V1.3-113, Chair of Risk, Safety and Uncertainty Quantification, ETH Zurich, Switzerland.

World Economic Forum (2016), "Shaping the Future of Construction A Breakthrough in Mindset and Technology", World Economic Forum: Cologny, Switzerland.

Yu, E., Skolnik, D., Whang, D.H. and Wallace, J.W. (2006), "Forced vibration testing of a four story RC building utilizing the nees@ucla mobile field laboratory", *Proceedings of the 8th U.S. National Conference on Earthquake Engineering*, San Francisco, CA, USA.